



# Signal detection in global mean temperatures after “Paris”: an uncertainty and sensitivity analysis

Hans Visser<sup>1</sup>, Sönke Dangendorf<sup>2</sup>, Detlef P. van Vuuren<sup>1,3</sup>, Bram Bregman<sup>4</sup> and Arthur C. Petersen<sup>5</sup>

5

<sup>1</sup> PBL Netherlands Environmental Assessment Agency, Bilthoven, The Netherlands

<sup>2</sup> Research Institute for Water and Environment, University Siegen, Siegen, Germany

<sup>3</sup> Faculty of Geosciences, University Utrecht, Utrecht, The Netherlands

10 <sup>4</sup> Institute for Science, Innovation and Society, Radboud University, Nijmegen, The Netherlands

<sup>5</sup> STEaPP, University College London, London, Great Britain

*Correspondence to:* Hans Visser ([hans.visser@pbl.nl](mailto:hans.visser@pbl.nl))

**Abstract.** In December 2015, 195 countries agreed in Paris to ‘hold the increase in global mean surface temperature (GMT) well below 2.0 °C above pre-industrial levels and to pursue efforts to limit the temperature increase to 1.5 °C’. Since large financial flows will be needed to keep GMTs below these targets, it is important to know how GMT has progressed since pre-industrial times, taking short-term and long-term (decadal) natural variability into account. However, the Paris Agreement is not conclusive as for methods to calculate it. Should trend progression be deduced from GCM simulations or from instrumental records by (statistical) trend methods? Which trend model should be chosen and what is ‘pre-industrial’? Does trend progression depend on the specific GMT dataset chosen? To find answers to these questions we performed an uncertainty and sensitivity analysis where datasets and model choices have been varied. For all cases we evaluated trend progression since pre-industrial, along with uncertainty information. To do so, we analysed four trend approaches and applied these to the five leading GMT products. As a parallel path, we calculated GMT progression from an ensemble of 106 GCM simulations, corrected for natural variability. We find GMT progression to be largely independent of various trend model approaches. However, GMT progression is significantly influenced by the choice of GMT datasets. Both sources of uncertainty are dominated by natural variability. Mean progression derived from GCM-based GMTs appears to lie within the range of the trend-dataset combinations. A difference between both approaches lies in the width of uncertainty bands: bands for GCMs are much wider. Results appear to be robust as for specific choices for ‘pre-industrial’. Our “Paris” policy recommendation would be to choose a spline or IRW trend model and estimate it on the average of the five leading GMT datasets, where 1880 is taken as base year. Given this choice trend progression for 2016 accounts for  $1.01 \pm 0.13$  °C (2- $\sigma$ ).

15  
20  
25  
30



## 1. Introduction

Global mean surface temperature (GMT) is undoubtedly one of the key indicators of climate change. Tollefson  
35 (2015) denotes the GMT indicator as ‘the global thermostat’. Over the years many articles have been published in  
relation to GMT series and the patterns therein. These patterns combine an anthropogenic signal – induced by  
growing concentration of greenhouses and processes such as aerosol cooling – as well as natural variability.  
Natural variability can be regarded as a correlated noise process consisting of (i) internal random unforced  
(chaotic) variability and (ii) external radiatively forced changes. Here, internal variability is steered by short-term  
40 processes such as weather in the high latitudes or El Niño and La Niña, as well as by decadal processes such as  
the Interdecadal Pacific Oscillation (IPO), and will result in correlated noise in GMTs (e.g., Trenberth, 2015; Fyfe  
et al. 2016; Xie, 2016; Meehl et al., 2016). Externally forced variability is mainly due to volcanic eruptions and  
variations in solar irradiance (IPCC, 2013; Forster et al., 2013; Mann et al., 2016). A recent realization of internal  
variability led to a fierce debate in the popular media: GMTs were showing a claimed “slowdown”, “pause” or  
45 “hiatus” from the year 1998 onwards (e.g., Lewandowski et al., 2015; Hedemann et al., 2017; Medhaug et al.,  
2017).

GMTs has become a crucial indicator in climate negotiations for a long time and even more so at the the 21th  
Conference of Parties (COP21) in Paris, December 2015. The final accord, approved by 195 countries, agreed on  
GMT targets which aim to avoid an increase of 1.5 and 2.0 °C compared to pre-industrial temperatures (UN, 2015).  
50 IPCC (2014a) showed that meeting such GMT targets will require deep reductions of GHG emissions at the cost  
of high investments in mitigation measures worldwide. Given the fact that all goals are formulated on the basis of  
this single GMT indicator, the question arises: what is the current GMT level since pre-industrial?

So far, little attention has been paid to this topic. IPCC (2013), in its attempt to clarify the meaning of GMT  
measurements, applied linear trends to three different GMT datasets. They report a trend progression  $\Delta\mu$  of 0.85  
55 [0.65, 1.06] °C over the period 1880-2012. The uncertainty range stands for 90% confidence limits, originating  
from differences in datasets, natural variability of the climate system (forced and unforced), and expert judgment.  
Hawkins et al. (2017) recently addressed the topic of trend progression since pre-industrial by quantifying the role  
of various choices for ‘pre-industrial’.

They found that the period 1720-1800 would be the most suitable in physical terms, despite incomplete  
60 information about radiative forcings and very few direct observations during this time. Additionally, they  
concluded that the 1850-1900 period would be a reasonable surrogate for pre-industrial GMTs by being only  
0,05 °C warmer than the 1720-1800 period. Subsequently, Hawkins et al. analysed GMT progression since pre-  
industrial by calculating the GMT mean over the 20-year period 1986-2005 for various GMT products and other  
instrumental data (their figure 4). Trend progression itself was approximated in the study by multiple regression  
65 models with non-stationary explanatory variables such as historic GHG forcing curves or local temperature series  
(the Central England Temperature series or the De Bilt series).



In this article we build on the work of Hawkins et al. but we do not base our GMT progression estimates on linear regression models with non-stationary regressors. The drawback of this approach is simply the linearity assumed, while the climate system is (highly) non-linear with a number of feedback processes. Therefore, we follow two other trend estimation approaches: (i) statistical trend models and (ii) global temperature trends derived from Global Climate Models (GCMs). Furthermore, we avoid methods or presentations based on subjectively selected time-windows (such as Moving Averages). The drawback of time windows is that averages over 20-year periods or alike do not give estimates for the beginning and ending of the sample period chosen.

Our approach is that of an uncertainty and sensitivity analysis as promoted by Saltelli et al. (2004), Saisana et al. (2005) and Visser et al. (2015). We ask the following two major questions:

- How robust are estimates for GMT progression since pre-industrial as for specific choices of trend modelling, use of GCMs and specific choices of GMT datasets?
- How do these choices influence uncertainties in GMT progression in relation to uncertainties due to natural variability?

Since there is no ‘true’ or ‘best’ trend approach (Visser et al., 2015), we explore four trend methods and apply these to five leading GMT products (similar to Hawkins et al.). This leads to a 4-by-5 matrix of GMT trend progressions since pre-industrial. As a parallel path we compare these trend progressions to those deduced from GCMs. We analyse an ensemble of 106 GCM experiments from the Coupled Model Intercomparison Project phase 5 (CMIP5), corrected for natural variability. Clearly, GCMs are fully physics-based, in contrast to trend methods, and it seems logical to give them priority in relation to the questions raised here. However, there are also drawbacks, the main being that GCMs are only approximations to the real climate system and have considerable biases. Although GCMs are tuned to meet the main characteristics of instrumental data (Voosen, 2016), GMTs derived from GCMs still show a wide range of trend-progression estimates, as we will show.

Our analysis is confined to historic data only (up to 2016). Examples for GMT projections have been given by IPCC (2013 - Ch. 12), Forster et al. (2013) and Mann (2014). A short-term prediction model is given by Suckling et al. (2016). Similarly, we will give an impression in section 6.2 how GMTs might evolve up to the year 2100, based on the historic trend progressions found here.



## 2 Data and methods

105

### 2.1 Data

Various research groups have published global GMT datasets. IPCC (2013 - section 2.4.3) used three datasets, namely the HadCRUT4 series (Morice et al., 2012; Hope, 2016), the NOAA dataset (Vose et al., 2012) and the  
110 NASA/GISS dataset (Hansen et al 2010). In the analysis here, we instead use a recent update of the NOAA data (Karl et al., 2015). Karl et al. applied a number of corrections which mainly deal with sea surface temperatures, such as the change from buckets to engine intake thermometers. In addition, we added two series, i.e. the version of the HadCRUT4 data in which the missing data have been filled in as published by Cowtan and Way (2014) and the GMT series by Rohde et al. (2013). Note that these datasets are not independent. They start from roughly the  
115 same station data over land, and more importantly are based on only two SST analyses: HadSST3 and ERSST v4. Cowtan and Way re-analysed the HadCRUT4 series by applying a statistical interpolation technique (Kriging) and satellite data for regions where data are sparse. Their series shows higher GMT values in recent decades than the non-interpolated HadCRUT4 series due to the more-than-average warming of the poles. The land part of the GMT data of Rohde et al. (2013; Berkeley Earth group of researchers) systematically addressed major concerns of global  
120 warming sceptics, mainly dealing with potential bias from data selection, data adjustment, poor station quality and the urban heat island effect. The ocean part (about 70%) is taken from HadSST3.

Since two out of five GMT products start in the year 1880, our analyses will use “1880” as pre-industrial for practical reasons. We return to this point in section 4. All data were downloaded from the institution websites with 2016 as the final year.

125 Next to these instrumental-data based GMTs we analyze three sets of GCM simulations all taken from CMIP5 (Taylor et al., 2012; IPCC, 2013 – Ch. 9-12). GMT is defined here as the global average of near-surface temperature, in contrast to the observational datasets that use SST over sea for practical reasons. The first set consists of GCM simulations where the input of greenhouse gases from 2005 onwards is taken from three Representative Concentration Pathways (RCPs): 4.5, 6.0 and 8.5 W/m<sup>2</sup> (Van Vuuren et al., 2011; IPCC, 2014 -  
130 section 12.4 and figure 12.5). These simulations cover the period 1861-2100. We have taken a set of 106 GCM simulations with one member per model. GCMs from CMIP5 are based on wide range of modeling differences such as climate sensitivities, cloud parametrization and aerosol forcing (e.g., IPCC 2013 - Ch. 9).

The second set that we have analyzed consists of 37 GCM runs for natural unforced variability, denoted as ‘historicalNat’. These runs comprise forced and unforced natural variability only (1860-2005). See Forster et al.  
135 (2013) for details. Finally, we analyzed 20 Pre-industrial Control (PiControl) runs of 200-year length. These runs simulate natural internal variability. All CMIP5 runs were downloaded from the KNMI Climate Explorer website with one member per model (Trouet and Van Oldenborgh, 2013).



## 2.2 Trend modeling

140

The tracking of signals or trends in GMT series has a long history, and a wide range of methods have been applied to isolate long-term signals or ‘trends’. We have summarized these in the Supplementary Material (table SM.1). As stated in the Introduction we choose statistical trend methods that allow for the quantification of trend progression where no window is needed and where uncertainty estimates are available for any incremental trend value. Furthermore, no specific period for pre-industrial has to be chosen (such as the mean of the 1851-1900 period or alike). ‘Pre-industrial’ is reflected in the choice of the start of the sample period only.

145

Based on these considerations we have selected four trend approaches for our sensitivity analysis: Ordinary Least Squares (OLS) linear trends, Integrated Random Walk (IRW) trends and two approaches with splines. The first trend - a linear fit by OLS - was chosen by IPCC (2013) as their main method. Uncertainties simply follow from the linear model:

150

$$\text{var}(\Delta\mu_{2016}) = \text{var}([a+b*2016] - [a+b*1880]) = 125^2 * \text{var}(b),$$

where ‘a’ is the intercept and ‘b’ the slope. The variance of ‘b’ follows from the OLS equations. Next to that the variance estimate is corrected by calculating effective sample sizes (IPCC, 2013 - 2SM). This correction is important since residuals are not white noise, mainly because the forcing is not linear but increases with time. A large part of the signal is therefore considered as noise with a large decorrelation scale in this approach.

155

The second trend approach that fulfils our uncertainty requirements, are sub-models from the class of Structural Time Series models (STMs), in combination with the Kalman filter (Harvey, 1989). From this group of models we choose the IRW trend model. The IRW trend model extends the linear regression trend line by a *flexible trend* while retaining all uncertainty information (Visser and Molenaar 1995; Visser, 2004; Visser et al., 2012; Visser et al., 2014; Visser et al., 2015). Furthermore, the flexibility of the trend model is optimized by Maximum Likelihood (ML) optimization. The Kalman filter is the ideal filter here since it yields the so-called Minimum Mean Squared Estimator (MMSE) for the trend component in the model. The Kalman filter has been applied in many fields of research and is gaining popularity in climate research recently (e.g., Hay et al., 2015).

160

165

A third and fourth approach applies a combination of a trend model and the statistical structure of natural internal variability as derived from PiControl runs. It can be seen as a hybrid approach. To do so we have chosen the cubic spline trend model, a trend approach also applied in the AR5 (IPCC, 2013 - Box 2.2, figure 1). Smoothing splines are not statistical in nature and, thus, do not generate uncertainty estimates for GMT increments  $\Delta\mu_{2016}$ . However, uncertainty bands can be reconstructed by Monte Carlo (MC) simulations under the assumption of a given mean, variance and autocorrelation structure estimated directly from the underlying dataset (figure 1 and Mudelsee 2014 - section 3.3). To steer the flexibility of the cubic spline model we studied the correlation structure of internal variability. This correlation structure can be described by an AutoRegressive Moving Average (ARMA)

170



175 model as proposed by Hunt (2011) and Roberts et al. (2015). They estimated ARMA models to a range of PiControl runs. Similarly, we analysed 20 PiControl runs and found that natural variability can reasonably be characterized by AR(1) processes where the AR(1) parameter  $\phi$  varies within the range [0.28 - 0.60], depending on the GCM run chosen (cf. Mudelsee, 2014 - section 2.1).

## 180 3 Results

### 3.1 Sensitivity analysis trend methods

185 Based on the 1880-2016 GMT sample period we have evaluated trend progression values  $\Delta\mu_{2016}$  from 1880 up to 2016 along with uncertainties for all datasets and trend approaches. This yields the 4-by-5 matrix shown in table 1. As for linear trends we corrected uncertainty estimates by a factor  $\sqrt{(1.60/0.40)} = 2.0$ , analogous to the approach chosen in IPCC (2013 - Ch. 2, Sup. Mat.) since first order autocorrelations lie around 0.60. Table 1 shows that the trend slopes for the dataset HadCRUT4, LOTI-NASA, NOAA-Karl and Cowtan and Way are close, where the lowest slope value is for the HadCRUT4 series. This dataset has poor coverage in the Arctic, where trends are  
190 much higher than the global mean. The steepest trend is found for the Berkeley Earth series, a remarkable result since the Berkeley Earth project was set-up to meet a range of critical comments from global warming sceptics. Identical patterns are found for the other trend models: lowest trend progression for the HadCRUT4 dataset and highest values for the Berkeley Earth dataset.

As for the IRW trend estimates we find reasonable flexible patterns which closely resemble the spline trend  
195 shown in IPCC (2013 - Ch.2: Box 2.2, Figure 1b). An example for the HadCRUT4 dataset is shown in figure 2. Data, trend and uncertainties are shown in the upper panel. The trend increments  $[\mu_t - \mu_{t-1}]$  and  $[\mu_t - \mu_{1880}]$  are given in the middle left and right panel, respectively, along with uncertainties. The  $[\mu_{2016} - \mu_{1880}]$  value with uncertainty is taken as value in table 1. The lower left panel shows the innovations or one-step-ahead predictions errors which follow from the Kalman filter formulae. The lower right panel shows the  
200 autocorrelation function (ACF). We note that a prerequisite of Kalman filtering is that the one-step-ahead prediction errors follow a white noise process. The ACF shows an AR(1) value of 0.30 which is slightly significant. Since the violation is small, we did not correct uncertainty ranges as we did for linear trends.

As for smoothing splines we have estimated trends in GMT series such that the residual series exhibits an AR(1) process with a  $\phi$  value of 0.28 and 0.60. Trend estimates based on the HadCRUT4 series are shown in figure 3.  
205 Both spline approaches show quite different trend patterns. The model shown in the upper panel of figure 3 is based on a slightly correlated noise process and - as for the IRW trend from figure 2 - closely resembles the spline trend shown in IPCC (2013 - Ch.2: Box 2.2, Figure 1b). The model shown in the lower panel shows a parabolic shape. This parabolic pattern closely resembles the anthropogenic signal in GMT series as shown by IPCC (2013 - figure 10.1f), derived from ‘historicalGHG’ simulation runs (Forster et al., 2013).



210 It is interesting to note that none of the four trend methods show a sign of a 'hiatus', 'slowdown' or 'pause'. That  
is not surprising for the linear trend and the spline estimate with  $\varphi=0.60$  due to their stiff character. However, the  
IRW trend and spline with  $\varphi=0.28$  are more flexible and do not show any stabilisation pattern for recent years at  
all. We tested the residuals of the IRW trend model and these appear to be close to white noise (cf. lower panels  
of figure 1). This inference is consistent with recent findings on the hiatus (e.g., Marotzke et al., 2015; Hedemann  
215 et al., 2017; Medhaug et al., 2017; Rahmstorf et al., 2017).

Table 1 shows is that differences between trend model and dataset combinations can be considerable. The  
lowest  $\Delta\mu_{2016}$  value is found for the HadCRUT4 dataset in combination with the IRW trend model:  $0.90 \pm 0.18^\circ\text{C}$   
( $\pm 2\text{-}\sigma$ ). The highest values are found for the Berkeley Earth dataset in combination with cubic spline interpolation  
and  $\varphi = 0.28$ :  $1.12 \pm 0.13^\circ\text{C}$ . These two extremes reveal that  $\Delta\mu_{2016}$  variability due to datasets and trend models  
220 accounts for  $0.22^\circ\text{C}$ . This variability is somewhat lower than variability due to natural variability alone. Based on  
 $2\text{-}\sigma$  limits, we find a low estimate of  $\pm 0.12^\circ\text{C}$  and a high estimate of  $\pm 0.19^\circ\text{C}$ , leading to a maximum ranges of  
 $0.24^\circ\text{C}$  (LOTI dataset in combination with cubic spline interpolation and  $\varphi = 0.28$ ) up to  $0.38^\circ\text{C}$  (LOTI dataset  
and OLS linear trend).

To quantify the role of trend methods in more detail we have averaged trend estimates over the five GMT  
225 datasets and added it to table 1 (bottom row). It shows that variability is small:  $[0.97, 1.01]^\circ\text{C}$ . At the other hand,  
if we average *over trend methods*, the variability due to datasets is found (right column of table 1). The variability  
accounts for  $[0.92, 1.09]^\circ\text{C}$ . Clearly, variability due to GMT datasets is dominant over specific trend approaches.

### 230 3.2 Trend progression derived from GCM simulations

Trend progression derived from GCMs have been analyzed in a range of studies, e.g. IPCC(2013 - Ch. 10), Forster  
et al. (2013), Marotzke and Forster (2016), Mann et al. (2016) and Meehl et al. (2016). Here, we derive trend  
progression since pre-industrial by taking an ensemble of 106 GCM all-forcing simulations 1861-2016. We note  
235 that underlying models have quite different characteristics. However, we did not perform an extensive sensitivity  
analysis as for these factors, as for example in Visser et al. (2000).

Short-term natural variability is smoothed by estimating splines to each individual simulation ( $\varphi = 0.28$  or,  
equivalently, 7 degrees of freedom, as in the upper panel of figure 3). In this way we find 106 values for  
 $\Delta_{i,2016} \equiv Y_{i,2016} - Y_{i,1880}$ , which are shown in the upper panel of figure 4. The mean  $\Delta_{2016}$  value is  $1.15 \pm 0.47^\circ\text{C}$   
240 ( $2\text{-}\sigma$ ). These values are consistent with those reported by Forster et al. (2013, table 3). Note that the GMT is defined  
slightly differently from the observational estimates, with near-surface temperatures rather than SSTs over sea  
areas. There are indications that this affects the trends and in fact explains the difference (Cowtan et al., 2016).  
Thus, strictly spoken, GMT values cannot be compared without accounting for this difference (and the difference  
in coverage for non-interpolated estimates such as HadCRUT4).





245 Since GCM simulations include externally-forced natural variability we remove forcings by volcanos and solar irradiation by analyzing an ensemble of 37 GCM simulations with natural forcing only ('historicalNat'; IPCC, 2013 - figures 10.1 and 10.7; Forster et al., 2013 - fig 2). The mean curve with 2 standard errors (SEs) is shown in the lower panel of figure 4, along with major volcanic eruptions (eruptions with a Volcanic Explosivity Index of 5 and 6). Mean trend progression for these 37 runs accounts for  $0.078 \pm 0.030$  °C (2-SE), 1861-2005.

250 Now, if we correct GCM simulations for natural forcings we find a mean progression  $\Delta_{2016}$  of  $1.07 \pm 0.47$  °C (2- $\sigma$ ).

#### 4 Discussion

255 The results shown in table 1 form the central findings in this study. Here, we make two comments concerning the robustness of these results. First, as summarized in table SM.1 of the Supplementary Material section, a wide range of trend models exist in the literature, all with varying characteristics. The fact that many of these methods are not statistical in nature does not limit their application in the present context: the approach shown in figure 1 (creating surrogate GMT series by MC simulation) is also applicable to methods such as binomial filters or LOESS  
260 estimators. Therefore, we cannot rule out that the influence of trend modelling is underestimated in table 1. However, given the (i) small differences shown in the bottom row of table 1, and (ii) the wide uncertainty bands due to natural variability, we judge such an under-estimation to be relatively small.

A second comment concerns a source of uncertainty not mentioned thus far, namely the choice for year or period that can be regarded as 'pre-industrial'. As for the analyses in section 3.1, we have chosen for the year 1880  
265 as low end of the sample period, simply because two out of five GMT products start in 1880 (NASA and NOAA). This choice is consistent with that made by IPCC (2013) as for historic trend progression (although some analyses are relative to 1850-1900). Would our results and conclusions from table 1 be different if the sample period would be enlarged, starting in 1720, 1850 or 1880?

Hawkins et al. (2017) have shown the difference between the two periods 1720-1800 and 1850-1900 to be  
270 small, around 0.05 °C. Additionally to their analysis we compared GMT mean values over three periods: 1850-1900, 1860-1880 and 1880-1900, based on the HadCRUT4 dataset. The mean values appear to be quite similar:  $-0.35 \pm 0.03$  °C,  $-0.35 \pm 0.06$  °C and  $-0.36 \pm 0.05$  °C, respectively (2- $\sigma$  limits). These differences are small if compared to the uncertainties due to natural variability, shown in table 1. We conclude that the choice for 1720-1800, 1850-1900 or 1880-1900 as 'pre-industrial' will not influence the findings presented here.

275 As for GCM-derived progressions we have taken the year 1861 as start of 'pre-industrial'. The reason for that choice is illustrated in the lower panel of figure 4. The period 1861-1880 is one with low volcanic activity, with only one volcanic eruption with a Volcanic Explosivity Index of 5. However, the period 1880-1900 is strongly influenced by eruptions, notably that of the Krakatoa with a VEI of 6. This eruption led to lowering of GMTs of





0.3 °C. Note that these volcanic signatures are **not** resembled in the instrumental data, probably due to poor  
280 coverage in the areas in which the signal would have been clearest, the tropics.

How do progression estimates shown in table 1 relate to GCM-derived trend progressions? In section 3.2 we  
estimated mean GCM progression, corrected for natural variability, to be  $1.07 \pm 0.47$  °C ( $2\text{-}\sigma$ ). These estimates  
appear to lie within the range of trend progressions based on instrumental data. E.g., they equal trend progression  
as derived from the Berkeley Earth dataset, which show trend progressions around  $1.06 \pm 0.14$  °C ( $2\text{-}\sigma$ ). Clearly,  
285 the uncertainty bands for instrumental trend estimates are much smaller.

We note that GMT trend estimates from instrumental data and GCMs are not independent. Modelling groups  
use various methods of tuning to relate their simulations to real world data (IPCC, 2013 - Ch 9; Voosen, 2016),  
although the very large spread indicates that they have not been very successful in tuning to the observed trend.

290

## 5 Conclusions and outlook

### 5.1 Conclusions

We have addressed the issue of signal progression of GMT in relation to the GMT targets agreed upon in Paris,  
December 2015. Although these targets are clearly defined - avoiding increments of 1.5 and 2.0 °C - there remain  
295 a number of (scientific) questions unanswered in the agreement. We have identified four aspects of the accord which  
hamper an exact quantification of GMT progression: (i) the use of instrumental data and trend methods versus  
GCM-derived progression, (ii) the role of varying datasets, (iii) the role of varying trend methods and (iv) the role  
of varying choices for pre-industrial. These questions are also relevant as GCM outcomes and their spread are used  
to make assessments on the efforts required to reach the Paris targets with a certain “likelihood”. Since there is no  
300 'true' or 'best' approach (Visser et al., 2015), we have chosen to perform an uncertainty and sensitivity on GMT  
progression as propagated by Saltelli et al. (2004) and related articles. This allows us to test the robustness of  
various trend progression claims.

As for approaches based on instrumental data we find that best guess values for GMT progression 1880-2016  
vary considerably, from 0.90 °C (HadCRUT4 dataset in combination with the IRW trend model) to 1.12 °C  
305 (Berkeley Earth dataset in combination with cubic spline interpolation and  $\phi = 0.28$ ). These two extremes reveal  
that  $\Delta\mu_{2016}$  variability due to datasets and trend models accounts for 0.22 °C. This variability is lower than  
variability due to natural variability alone. Based on  $2\text{-}\sigma$  limits, we find a low estimate of 0.24 °C (LOTI dataset  
in combination with cubic spline interpolation and  $\phi = 0.28$ ) and a high estimate of 0.38 °C (LOTI dataset and  
OLS linear trend). Furthermore, variability due to various GMT products dominates the variability due to specific  
310 trend approaches.



As for approaches based on GCMs we find that mean trend progressions lies within the range of estimates from instrumental data. However, the uncertainty bands for 106 simulations are much wider than those derived from instrumental trend estimates. Here, GCM variability stems from a wide range of modeling assumptions such as climate sensitivities, cloud parameterization and aerosol forcing (e.g., IPCC, 2013 - Ch. 9), rather than from natural  
315 variability.

As a side result of our trend analyses we note that no signs of an 'hiatus', 'slowdown' or 'pause' can be discerned GMT trend progression. This inference is consistent with recent findings, e.g. Marotzke et al. (2015), Hedemann et al. (2017), Medhaug et al. (2017) and Rahmstorf et al. (2017).

## 320 5.2 Outlook

The results presented here, have relevance for upcoming climate negotiations. If countries would agree to follow the *precautionary principle* with respect to the uncertainty topics raised in this paper, the best choice for datasets is the GMT dataset published by the Berkeley Earth project: trend progression is highest for this dataset (sixth row in table 1):  $1.12 \pm 0.13$  °C (2- $\sigma$ ). If countries would agree to follow a best-guess value which is robust against the  
325 factors addressed here, we propose to choose the IRW or spline trend trend model and to apply it on the average of five leading GMT products (for psychological reasons all datasets are chosen as equally important). For this choice trend progression accounts for  $1.01 \pm 0.13$  °C. Although estimates based on GCMs are consistent with this estimate, as shown above, GCM simulations are not a logical choice here due to their wide spread (cf. upper panel in figure 4).

330 To give an impression how GMTs might evolve in the future, we have calculated two mean GCM projections: one based on the RCP2.6 scenario (32 simulations) and one based on the RCP4.5 scenario (42 simulations). All simulations are contained in the 106 GCM simulations used in section 3.2, and scaled to have a mean value of 1.01 °C in the year 2016 (the mean value of historic trend progression as derived above). See figure 5.

We find that, if countries are able to reduce GHG emissions according to the RCP2.6 scenario, best guess GMT  
335 values will stay below the 1.5 °C target. Under unfavourable circumstances this target could be reached by the year 2040. The 2.0 °C target is never reached. Under the RCP4.5 emission scenario both temperature targets are reached before the year 2100, even under favourable conditions.

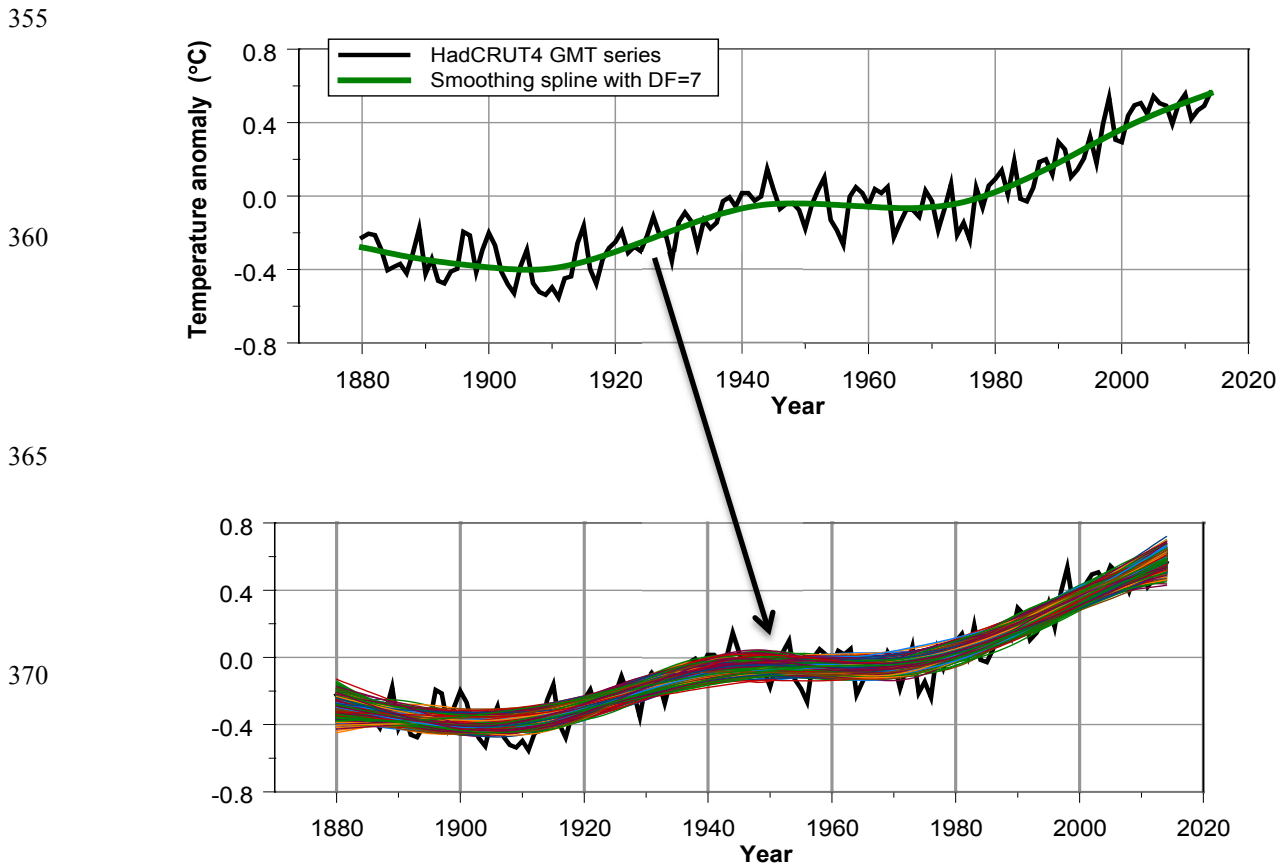


340 **Table 1.** Trend increments  $\Delta\mu_{2016}$  along with 2- $\sigma$  confidence limits. Increments are given for five GMT series and four trend approaches.

GMT dataset	GMT progression $\Delta\mu_{2016}$ with 2- $\sigma$ confidence limits (°C)				
	OLS linear trend	IRW trend	Spline with $\phi=0.28$	Spline with $\phi=0.60$	Mean progression
<b>HadCRUT4, CRU</b>	0.90 (± 0.18)	0.93 (± 0.13)	0.94 (± 0.12)	0.92 (± 0.14)	0.92
<b>HadCRUT4, Cowtan and Way</b>	0.96 (± 0.17)	1.06 (± 0.13)	1.06 (± 0.12)	0.98 (± 0.15)	1.02
<b>LOTI series, NASA</b>	0.98 (± 0.19)	1.02 (± 0.14)	1.01 (± 0.12)	0.99 (± 0.14)	1.00
<b>Karl <i>et al</i> (2015), NOAA</b>	0.95 (± 0.19)	0.96 (± 0.15)	0.94 (± 0.14)	0.95 (± 0.14)	0.95
<b>Berkeley Earth Project</b>	1.04 (± 0.17)	1.12 (± 0.13)	1.12 (± 0.13)	1.06 (± 0.14)	1.09
<b>Mean progression</b>	0.97	1.02	1.01	0.98	1.00

345

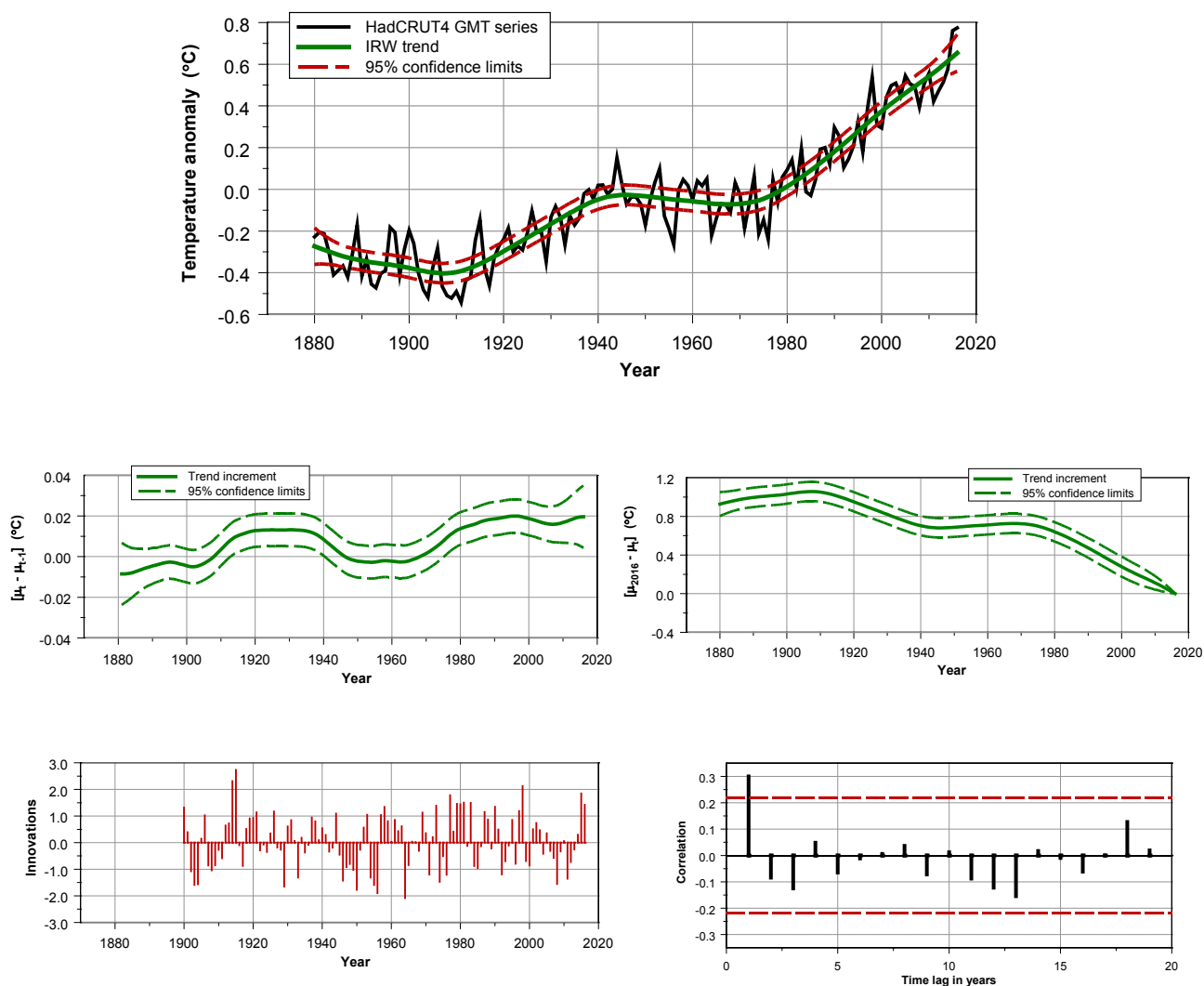
350



375

**Figure 1.** Construction of 1000 surrogate trend series by MC simulation, based on cubic splines. The AR(1) parameter estimated on the residuals of the spline model in the upper panel, accounts for 0.28. A surrogate GMT series  $\hat{y}_{i,t}$  is formed by simulating a new residual series  $r_{i,t}$  based on the AR(1) process with  $\phi=0.28$ , and adding it to the estimated spline (green line upper panel). Then, a spline trend  $\mu_{i,t}$  is estimated for each surrogate  $\hat{y}_{i,t}$ . As an illustration we have plotted 1000 of such trends  $\mu_{1,t}, \dots, \mu_{1000,t}$  in the lower panel. Now, confidence limits can be estimated for any  $\mu_t$  based on the values  $\mu_{1,t}, \dots, \mu_{1000,t}$ . These confidence limits can be based on standard deviations or percentiles. Similarly, confidence limits can be calculated for the increment  $[\mu_{2016} - \mu_{1880}]$ , based on the values  $[\mu_{1,2014} - \mu_{1,1880}], \dots, [\mu_{1000,2014} - \mu_{1000,1880}]$  (Mudelsee, 2014 - Sections 3.3.3 and 3.4).

380



385

**Figure 2.** Results for the IRW trend model as applied to the HadCRUT4 series. Period: 1880-2016. The upper panel shows the trend (green line) along with 95% confidence limits (red dashed lines). The trend increments  $[\mu_t - \mu_{t-1}]$  are given in the middle left panel along with uncertainties. Idem the  $[\mu_t - \mu_{1880}]$  values in the middle right panel. The lower left panel shows the innovations or one-step-ahead predictions errors which follow from the Kalman filter formulae. The lower right panel shows the autocorrelation function (ACF).

390

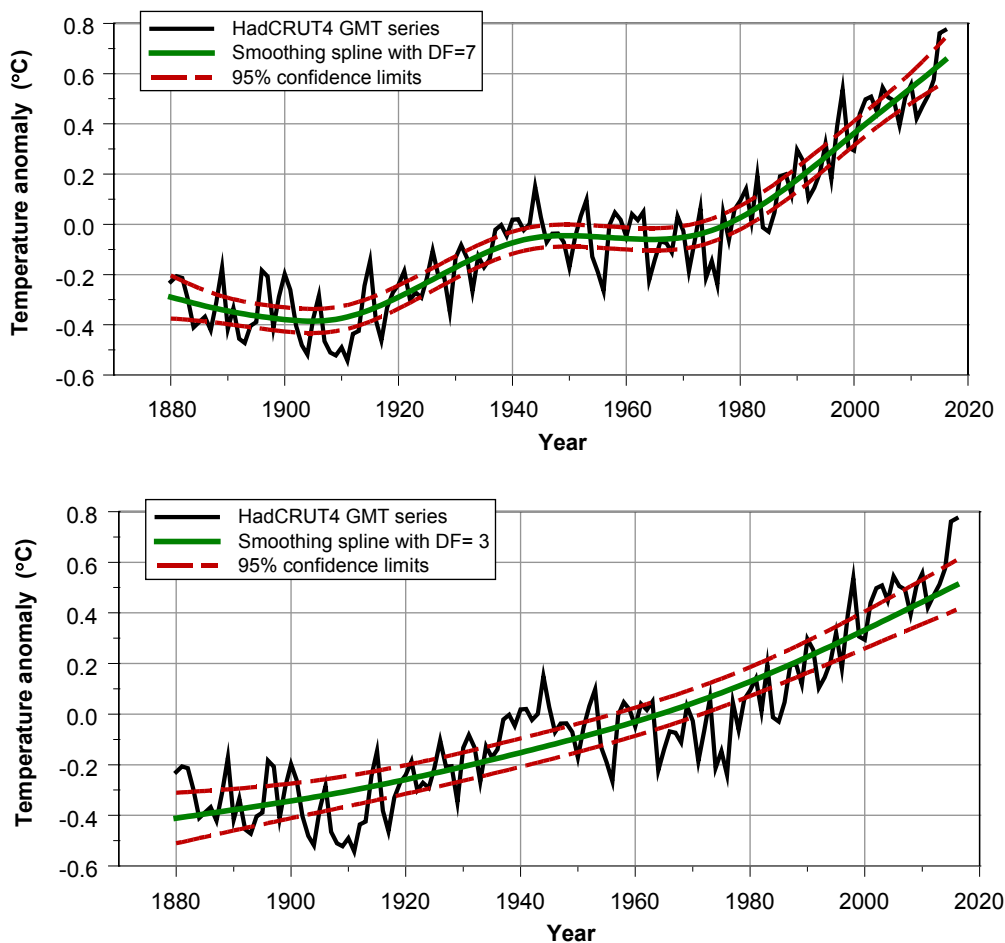
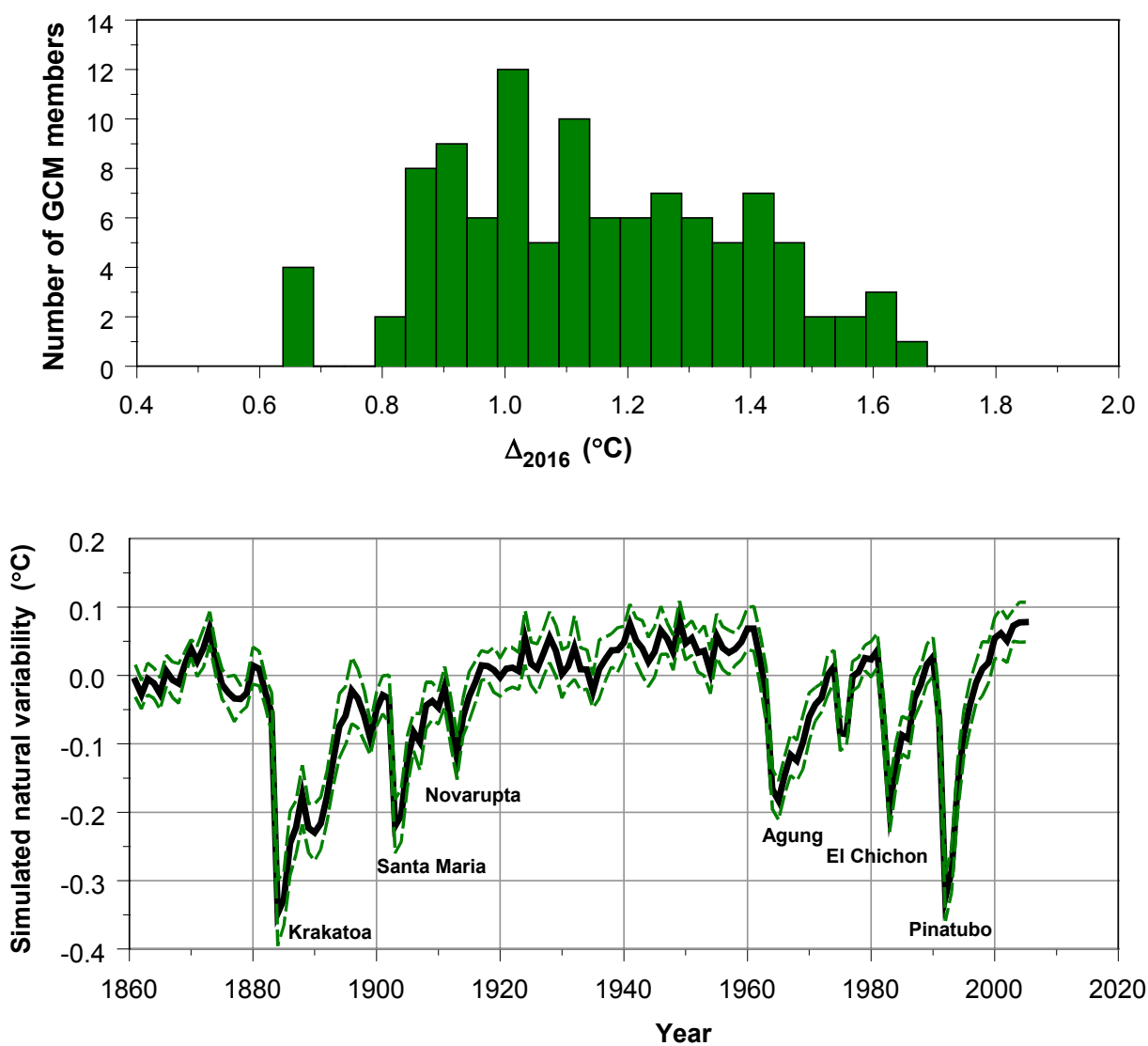


**Figure 3.** Two smoothing spline estimates for the HadCRUT4 GMT series, with uncertainties generated by MC simulation. All confidence limits are based on 1000 surrogate GMT series following the approach set out in Mudelsee (2014 - Section 3.3.3). Upper panel: AR(1) parameter chosen as  $\varphi = 0.28$  (equivalent to 7 degrees of freedom), the low end of  $\varphi$  values within CMIP5 PiControl runs. Lower panel: AR(1) parameter chosen as  $\varphi = 0.60$ , the high end of  $\varphi$  values (DF=3).

400



405 **Figure 4.** Upper panel: histogram based on 106 GCM  $\Delta_{i,2016}$  values. Mean value is  $1.15 \pm 0.47$  °C ( $2\sigma$ ). Individual GCM curves were smoothed by splines. Lower panel: natural variability based on 37 GCM simulations. Shown are mean values along with 2 standard errors. Period is 1861-2005.



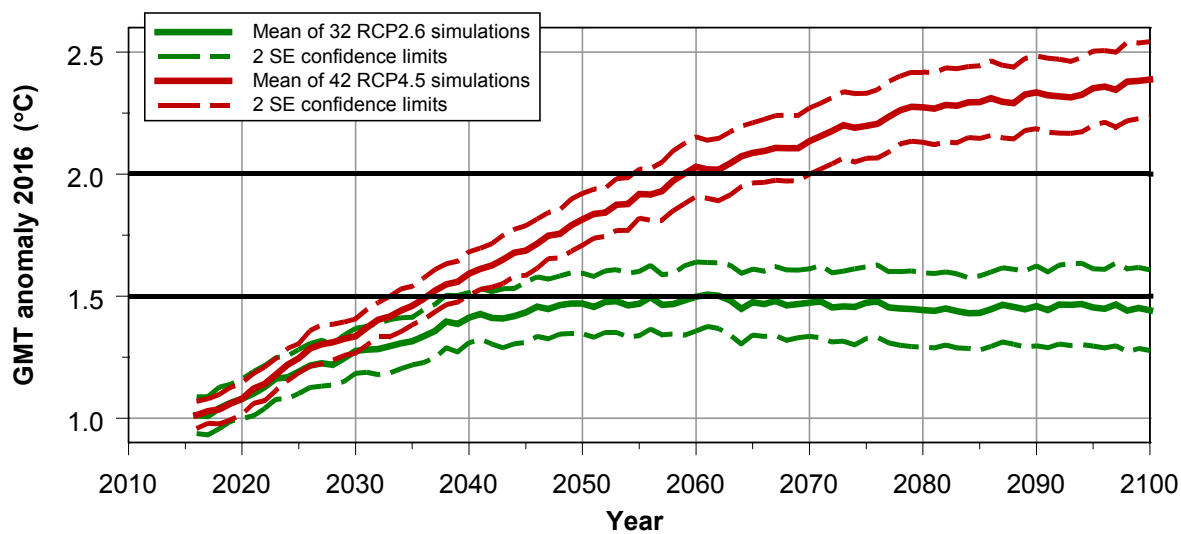


**Figure 5.** Mean GMT projections based on the RCP2.6 emission scenario (32 simulations, green lines) and based on the RCP4.5 emission scenario (42 simulations, red lines). Both mean curves are shifted such that 2016 values account for 1.01 °C. Uncertainty limits are based on 2 Standard Errors (SEs).



420 **Code availability.** IRW trends have been estimated by the TrendSpotter software. This software package is freely available from the first author. Splines have been estimated by the statistical package S-Plus, version 8.2. The scripts which are highly similar to R, are available from the first author.

**Data availability.** All five GMT datasets are open access and have been downloaded from the authors websites.  
425 All CMIP5 runs named in Section 2.1 were downloaded from the KNMI Climate Explorer website with one member per model (Trouet and Van Oldenborgh, 2013). The names of individual GCMs can be found there as well. Please see [https://climexp.knmi.nl/cmip5\\_indices.cgi?id=someone@somewhere](https://climexp.knmi.nl/cmip5_indices.cgi?id=someone@somewhere). Data used for the graphical presentations in this article can be gained from the first author.

430 **The Supplement related to this article is available online**

**Competing interests.** The authors declare that they have no conflict of interest.

**Acknowledgments.** We thank Geert Jan van Oldenborgh (KNMI, Climate Explorer) for thorough comments on an early version of this text.

435

440



## References

- 445 Climate Analytics: The 1.5 °C temperature limit in the Paris Agreement and 2016 temperature records, Briefing paper, 2016.
- Cowtan, K. and Way, R. G.: Coverage bias in the HadCRUT4 temperature series and its impact on recent temperature trends, *Q.J.R. Meteor. Soc.*, 140, 1935-1944, 2014.
- Cowtan, K., Hausfather, Z., Hawkins, E., Jacobs, P., Mann, M.E., Miller, S. K., Steinman, B. A., Stolpe, M. B.  
450 and Way, R. G.: Robust comparison of climate models with observations using blended land air and ocean sea surface temperatures, *GRL*, doi:10.1002/2015GL064888 6527-6534, 2016.
- Forster, P.M., Andrews, T., Good, P., Gregory, P.M., Jackson, L. S., Zelinka, M.: Evaluating adjusted forcing and model spread for historical and future scenarios in the CMIP5 generation of climate models, *JGR: Atmospheres* 118, 1139-1150, 2013.
- 455 Fyfe, J. C., Meehl, G. A., England, M. H., et al: Making sense of the early-2000s warming slowdown, *Nature Climate Change*, 6, 224-228, 2016.
- Hansen, J., Ruedy, R., Sato, M. and Lo, K.: Global surface temperature change, *Reviews of Geophysics*, 48, RG4004, 2010.
- Harvey A.C.: Forecasting, structural time series models and the Kalman filter, Cambridge University Press,  
460 Cambridge United Kingdom, 1989.
- Hawkins, E., Ortega, P., Suckling, E., Schurer, A., Hegerl, G., Jones, P., Joshi, M., Osborn, T., Masson-Delmotte, V., Mignon, J., Thorne, P. and Van Oldenborgh, G.: Estimating changes in global temperature since the pre-industrial period, *Bull. Amer. Meteor. Soc.*, doi:10.1175/BAMS-D-16-0007, preliminary version on Internet, 2017.
- 465 Hay, C.C., Marrow, E., Kopp, R. E. and Mitrovica, J.X.: Probabilistic reanalysis of twentieth-century sea-level rise, *Nature*, 517, 481–484, 2015.
- Hedemann, C., Mauritsen, T., Jungclaus, J., Marotzke, J.: The subtle origins of surface-warming hiatuses, *Nature Climate Change*, 7, 336-339, 2017.
- Hope, M.: Temperature spiral goes viral, *Nature Climate Change*, 6, 657, 2016.
- 470 Hunt, B.G.: The role of natural climatic variation in perturbing the observed global mean temperature trend, *Clim. Dyn.*, 36, 509-521, 2011.
- IPCC: Climate Change 2013: the Physical Science Basis. Contribution of Working Group I to the Fifth Assessment Report of the Intergovernmental Panel on Climate Change [Stocker, T. F., Qin, D., Plattner G. K., et al. (eds)] Cambridge: Cambridge University Press, 2013.
- 475 IPCC: Climate Change 2014: Mitigation of climate change. Contribution of Working Group III to the Fifth Assessment Report of the Intergovernmental Panel on Climate Change [Edenhofer, O., Pichs-Madruga, R. et al. (eds)] Cambridge: Cambridge University Press, 2014a.



- IPCC: Climate Change 2014: Synthesis Report. Contribution of Working Groups I, II and III to the Fifth Assessment Report of the IPCC [Pechauri, R. K. and Meyer, L. A. (eds)] IPCC Geneva, Switzerland, 2014b.
- 480 Karl, T. R., Arguez, A., Huang, B., et al: Possible artifacts of data biases in the recent global surface warming hiatus, *Science*, 348, 1469-1472, 2015.
- Kosaka, Y. and Xie, S.P.: Recent global-warming hiatus tied to equatorial Pacific surface cooling, *Nature*, 501, 403-408, 2013.
- 485 Lewandowsky, S., Oreskes, N., Risbey, J. S., Newell, B. R.: Seepage: climate change denial and its effect on the scientific community. *Global Environm. Change*, 33: 1-13, 2015.
- Mann, M. E.: Earth will cross the climate danger threshold by 2036, *Scientific American*, April issue, 2014.
- Mann, M. E., Rahmstorf, S., Steinman, B. A., Tingley M. and Miller, S.K.: The likelihood of recent record warmth, *Nature Scientific Reports*, DOI:10.1038/srep19831, 2016.
- 490 Marotzke, J., Forster, P. M.: Forcing, feedback and internal variability in global temperature trends, *Nature*, 517, 565-570, 2015.
- Medhaug, I., Stolpe, M. B., Fischer, E. M. and Knutti, R.: Reconciling controversies about the 'global warming hiatus', *Nature*, 545, 41-47, 2017.
- Meehl, G. A., Hu, A., Santer, B. D. and Xie, S-P: Contribution of the Interdecadal Pacific Oscillation to twentieth-century global surface temperature trends, *Nature Climate Change*, 6, 1005-1008, 2016.
- 495 Morice, C. P., Kennedy, J. J., Rayner, N. A. and Jones, P.D.: Quantifying uncertainties in global and regional temperature change using an ensemble of observational estimates: the HadCRUT4 data set, *J. of Geophys. Res.*, 117, doi:10.1029/2011JD017187, 2012.
- Mudelsee, M.: *Climate time series analysis: classical statistical and bootstrap methods*, Springer, New York, USA, 2014.
- 500 Rahmstorf, S., Forster, G. and Cahill, N.: Global temperature evolution: recent trends and some pitfalls, *Environ. Res. Lett.*, 12, 054001, 2017.
- Roberts, C. D., Palmer, M. D., McNeall, D., Collins, M.: Quantifying the likelihood of a continued hiatus in global warming, *Nature Clim. Change*, doi:10.1038/NCLIMATE2531, 2015.
- 505 Rohde, R., Muller, R., Jacobsen, R., Perlmutter, S., Rosenfeld, A., Wurtele, J., Curry, J., Wickham, C., Mosher, S.: Berkeley Earth temperature averaging process, *Geoinformatics & Geostatistics: An Overview 1/2*, 1-13, 2013.
- Saisana, M., Saltelli, A., Tarantola, S.: Uncertainty and sensitivity analysis techniques as tools for the quality assessment of composite indicators, *J. R. Statist. Soc. A*, 168, 307-323, 2005.
- 510 Saltelli, A., Tarantola, S., Campolongo, F. and Ratto, M.: *Sensitivity analysis in practice* Wiley & Sons, Chichester UK, 2004.
- Suckling, E. B., Van Oldenborgh, G. J., Eden, J. M. and Hawkins, E.: An empirical model for probabilistic decadal prediction: global attribution and regional hindcasts, *Clim Dyn*, doi:10.1007/s00382-016-3255-8, 2016.



- 515 Taylor, K. E., Stouffer, R.J., Meehl, G. A.: An overview of CMIP5 and the experiment design, BAMS april issue, 485-498, 2012.
- Thomson, A. M. et al: RCP4.5: a pathway for stabilization of radiative forcing by 2100, *Clim. Change*, 109,77-94, 2011.
- Tollefson, J.: The 2 °C dream, *Nature* 527, 436-438, 2015.
- Trenberth, K. E.: Has there been a hiatus? *Science*, 349, 691-692, 2015.
- 520 Trouet, V. and Van Oldenborgh, G. J.: KNMI Climate Explorer: a web-based research tool for high-resolution paleoclimatology, *Tree-Ring Research*, 69(1), 3-13, 2013.
- UN: Adoption of the Paris Agreement. FCCC/CP/2015/L.g/Rev.1, 2015.  
<http://unfccc.int/resource/docs/2015/cop21/eng/l09r01.pdf>
- 525 Van Vuuren, D., Edmonds, J., Kainuma M., et al: The representative concentration pathways: an overview, *Clim. Change*, 109, 5-31, 2011.
- Visser, H.: Estimation and detection of flexible trends, *Atmosph. Environ.* 38, 4135-4145, 2004.
- Visser, H. and Molenaar, J.: Trend estimation and regression analysis in climatological time series: an application of structural time series models and the Kalman filter, *J. of Climate*, 8(5), 969-979, 1995.
- 530 Visser H, Folkert R. J. M., Hoekstra J. and De Wolf J. J.: Identifying key sources of uncertainty in climate change projections, *Clim. Change*, 45, 421-457, 2000.
- Visser, H. and Petersen, A.C.: Inferences on weather extremes and weather-related disasters: a review of statistical methods, *Clim. of the Past*, 8, 265-286, 2012.
- 535 Visser, H., Petersen, A. C. and Ligtoet W.: On the relation between weather-related disaster impacts, vulnerability and climate change, *Clim. Change*, 125, 461-477, 2014.
- 540 Visser, H., Dangendorf, S., Petersen, A.C.: A review of trend models applied to sea level data with reference to the “acceleration-deceleration debate”, *J. of Geophys. Res.: Oceans*, 120, 3873-3895, doi:10.1002/2015JC010716, 2015.
- Voosen, P.: Climate scientists open up their black boxes to scrutiny, *Science*, 354, 401-402, 2016.
- Vose RS et al.: NOAA’s merged land-ocean surface temperature analysis, *Bull. Am. Meteor. Soc.*, 93, 1677- 1685, 2012.
- Xie, S. P.: Leading the hiatus research surge, *Nature Clim. Change*, 6, 345-346, 2016.

545